

# X-ray magnetic linear dichroism as a probe for non-collinear magnetic state in ferrimagnetic single layer exchange bias systems

Chen Luo<sup>1,2,3,\*</sup>, Hanjo Ryll<sup>1</sup>, Christian H. Back<sup>2,3</sup>, and Florin Radu<sup>1,\*\*</sup>

<sup>1</sup>Helmholtz-Zentrum-Berlin für Materialien und Energie, Albert-Einstein-Strasse 15, 12489 Berlin, Germany

<sup>2</sup>Institute of Experimental and Applied Physics, University of Regensburg, 93053 Regensburg, Germany

<sup>3</sup>Institute of Experimental Physics of Functional Spin Systems, Technical University Munich, James-Franck-Str. 1, 85748 Garching b. München, Germany

\* [chen.luo@ur.de](mailto:chen.luo@ur.de)

\*\* [florin.radu@helmholtz-berlin.de](mailto:florin.radu@helmholtz-berlin.de)

November 14, 2018

## Abstract

Ferrimagnetic alloys are extensively studied for their unique magnetic properties leading to possible applications in perpendicular magnetic recording, due to their deterministic ultrafast switching and heat assisted magnetic recording capabilities. On a prototype ferrimagnetic alloy we demonstrate fascinating properties that occur close to a critical temperature where the magnetization is vanishing, just as in an antiferromagnet. From the X-ray magnetic circular dichroism measurements, an anomalous 'wing shape' hysteresis loop is observed slightly above the compensation temperature. This bears the characteristics of an intrinsic exchange bias effect, referred to as *atomic exchange bias*. We further exploit the X-ray magnetic linear dichroism (XMLD) contrast for probing non-collinear states which allows us to discriminate between two main reversal mechanisms, namely perpendicular domain wall formation versus spin-flop transition. Ultimately, we analyze the elemental magnetic moments for the surface and the bulk parts, separately, which allows to identify in the phase diagram the temperature window where this effect takes place. Moreover, we suggest that this effect is a general phenomenon in ferrimagnetic thin films which may also contribute to the understanding of the mechanism behind the all optical switching effect.

Non-collinear magnetism is emerging as a crucially important trait of magnetic systems which are indispensable to antiferromagnetic spintronics [1]. Magnetic skyrmions, helical and conical states, canted spins specific to frustrated systems, domain walls in ferromagnetic and antiferromagnetic materials are all attempted to be controlled through external stimuli (electric currents, voltages, laser excitations, strain) towards functionalization for applications in modern devices. Moreover, non-collinear spin textures in ferrimagnets can give rise to anomalous Hall effect [2, 3], which enables readout in magnetic sensors. While important progress is made on the understanding of complex magnetic textures in single crystals, the miniaturization of devices requires nano-scaling of the materials, which leads to significant modifications of their bulk magnetic properties.

Among magnetic materials, rare-earth-transition-metals (RE-TM) ferrimagnetic alloys have attracted great interest because they exhibit superior flexibility in designing desired properties for

ultimate functionality and as model systems for basic research in the field of spintronics. They can be easily engineered as two ferromagnetic oppositely oriented sub-lattices in form of thin films and nanostructures with controllable perpendicular anisotropy, variable net magnetization as a function of stoichiometry and tunable spin reorientation transition temperature [4]. They can also be assembled as heterostructures in form of spin valves and tunnel junctions [5, 6]. For example, DyCo/Ta/FeGd has been demonstrated to exhibit interlayer exchange coupling and a tunable and robust perpendicular exchange bias at room temperature, which can be set without additional field cooling cycles [5, 4]. The DyCo<sub>5</sub> material has also been proposed to be suitable for heat-assisted magnetic recording near room temperature [7]. For the archetypical GdFeCo and other RE-TM ferrimagnets like TbFe, TbCo it has been demonstrated that their magnetization can be controlled using femtosecond laser pulses at large lateral length scales and at the nanoscale, without applying any external magnetic field [8, 9, 10, 11, 12]. RE-TM ferrimagnetic alloys can be tuned to behave as true antiferromagnets at a compensation temperature where the magnetic moments of the RE and TM sub-lattices are equal in size but oppositely oriented, leading to a zero net magnetization. For some RE elements with low orbital magnetic moments, comparable to the orbital magnetic moment of the TM element, the angular momentum may be quenched for a certain temperature which may lead to an acceleration of the precessional spin dynamics [13, 14]. Ultrafast magnetization reversal across the compensation temperature of RE-TM alloys may deterministically provide the ultimate switching speeds that can be achieved today [15, 16, 17, 18, 19].

The complex physics near the compensation temperature is enriched by one more fascinating effect. Anomalous magnetic behavior in form of *wing shape* hysteresis loop has been reported in several RE-TM ferrimagnetic alloys that exhibit a perpendicular magnetic anisotropy such as, GdCo [20], HoCo [21], TbFe [22], GdFe [23], DyCo<sub>4</sub> [24], and GdFeCo [25, 26, 27] thin films. When applying a magnetic field perpendicular to the sample, it is expected that the net magnetization will naturally align with the external field. However, a counter-intuitive effect is observed: the magnetization diminishes when the magnetic field overcomes a certain value, leading to a decrease or even a vanishing magnetization of the sample.

Originally, this intriguing effect was interpreted based on models assuming an alloy composition gradient across the film thickness or even across lateral directions of the sample. According to these assumptions, a compensation temperatures range will occur and, as a result the magnetic hysteresis loop will reflect the relative weight of the corresponding "below" and "above" compensation parts of the film [20, 25]. These early models have been addressed critically in relation to similar observations in HoCo films [21], questioning the original proposals based on the structural or magnetic inhomogeneities. Recently, the observation of similar anomalous loops in GdFeCo was observed to occur at faster time scales [23]. For this case the origin for the effect was suggested to be caused by a transient temperature range which extends over the compensation temperature of the film. Even more recently, similar anomalous magnetic behavior in the same GdFeCo films was reported in equilibrium with the suggestion that its origin actually may relate to a spin-flop mechanism [27]. This last attempt to resolve the debate, however, comes at odds with previous observation of this effect in a DyCo<sub>4</sub> film where it is suggested that the effect bears the characteristics of an exchange bias effect [24]. As a result, although this effect is of paramount importance for ultrafast magnetization research, its fundamental origin is still highly debated. We center our study on resolving the origin of the effect utilizing one of the most powerful modern experimental tools to magnetism, namely soft x-ray spectroscopy. Moreover, we suggest that this effect may explain the origin of all optical switching in ferrimagnetic films (see Discussion section and Supplementary).

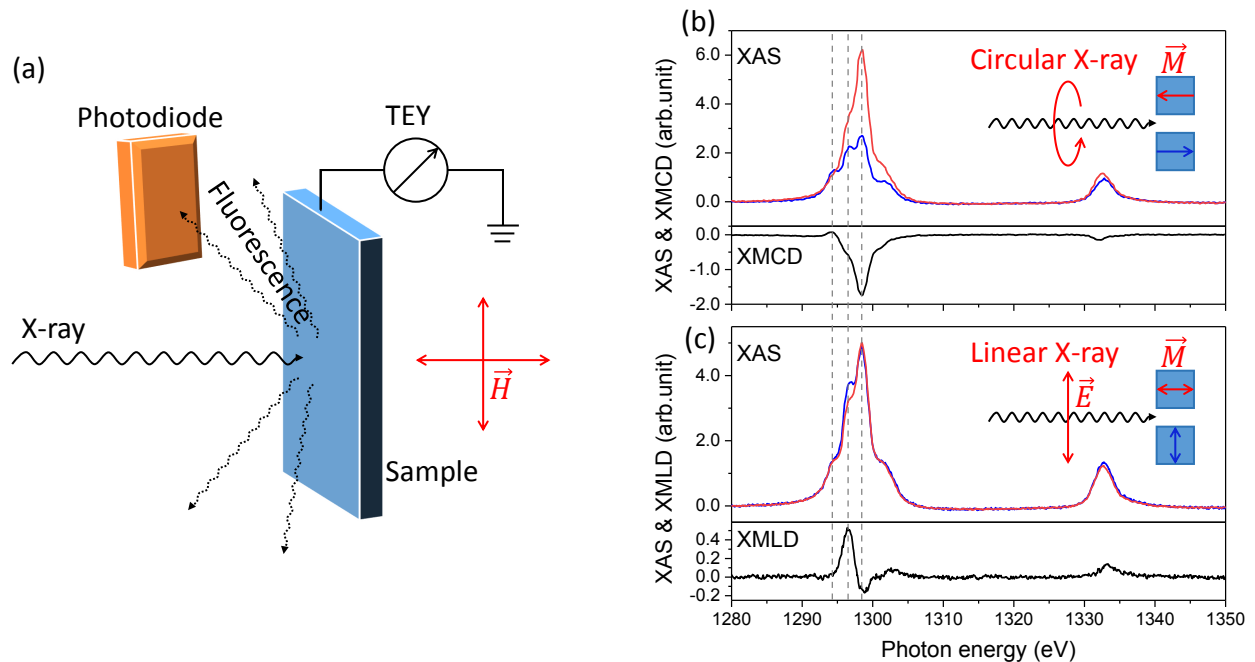


Figure 1: (a) Sketch of the XMCD and XMLD measurements, the fluorescence and TEY signals from the sample are recorded. (b) The XAS and XMCD spectra for the Dy  $M_{4,5}$  edges at 300 K. (c) The XAS and XMLD spectra for the Dy  $M_{4,5}$  edges at 300 K. The three peaks of Dy  $M_5$  edge are marked by the dashed lines at  $E = 1294.3$ ,  $1296.5$  and  $1298.4$  eV. The data in panels (b) and (c) were both recorded in FY mode.

## Results

We make use of x-ray circular magnetic dichroism (XMCD) [28] and x-ray linear magnetic dichroism (XMLD) assembled from magnetic field dependent absorption spectra (XAS) measured by total electron yield (TEY) and by fluorescence yield (FY) to resolve the origin of the magnetic transition that occurs close to the compensation temperature of RE-TM ferrimagnetic alloys. XMCD is sensitive to the ensemble averaged orbital and spin contribution to the magnetic moments projected along the circular polarization direction which is set to be parallel to the x-ray beam direction. Through the sign of XMCD one can distinguish the directional sense of the magnetic moments. However, through its magnitude one cannot uniquely discriminate on their eventual non-collinear arrangement with respect to magnetic domain formation. To achieve this capability, the XMLD contrast will be involved.

XMLD [29, 30, 31, 32, 33] is the difference in XAS cross section for the  $\vec{E}$  vector of linear polarized X-rays oriented parallel and perpendicular to the magnetic moments. XMLD depends on the square of the magnetic moment  $\langle M^2 \rangle$  and on the magneto-crystalline anisotropy, which makes it favorable for the study of antiferromagnetic systems. In spite of the key dependences to intrinsic magnetic properties, for 3d transition metal elements (Mn, Co, Fe) the size of the XMLD effect is extremely small, hindering its further development [31, 34]. Also, it requires a rather high precision of reproducibility of energy set since the size of its sign changing contrast at the  $L_3$  resonant edge occurs in a narrow energy range. We exploit here, as demonstrated further below, the XMLD at the RE (Dy) edges which is expected to be much larger [29] and occurs as a sizable intensity change at the  $M_5$  edge for both TEY and FY detection modes.

First we present the demonstration of XMCD and XMLD geometries and the novel characteristics of the XMLD effect at the Dy M edges through an experiment to probe the non-collinear states in  $\text{DyCo}_5$  ferrimagnetic thin films at room temperature. Figure 1(a) shows the experimental

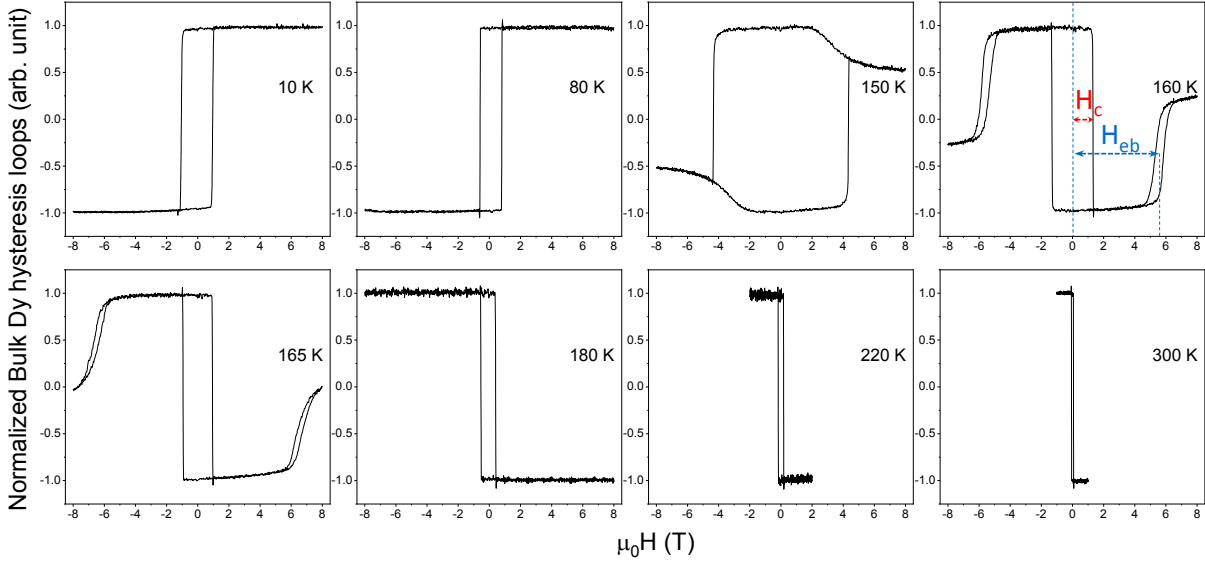


Figure 2: Temperature dependent hysteresis loops recorded by FY signal with circular polarized X-rays set to the Dy  $M_5$  edge ( $E = 1298.4$  eV). The shift of the side hysteresis loop denoted as  $H_{cb}$  and the coercive field of the central loop denoted as  $H_c$  are depicted schematically in the top-right panel.

geometry for the surface and bulk measurements (see also Supplementary). All the measurements were performed in a perpendicular geometry, the bulk sensitive FY signal with a probing depth of  $\sim 100$  nm [35] was recorded by a photodiode located 2 cm away from the sample surface. Fig. 1(b) shows the XAS and XMCD measurements for Dy at 300 K. The XMCD spectrum was obtained by taking the difference of  $(\sigma^+ - \sigma^-)$ , where  $\sigma^+$  and  $\sigma^-$  represent the XAS spectra measured by FY and using the circular polarized X-rays with the magnetic field ( $\mu_0 H = 1$  Tesla) parallel and anti-parallel to the beam direction. The Dy XMLD spectrum was obtained by taking the difference of the XAS spectra measured by keeping the linear polarized X-rays  $\vec{E}$  parallel to the synchrotron plane and perpendicular to the beam direction, and setting the direction of the magnetic moments perpendicular and parallel to  $\vec{E}$ , respectively, as shown in Fig. 1(c). The magnetic field of 1 Tesla was checked to saturate the magnetization of the sample whether in-plane or out-plane at room temperature. The field was applied parallel to the beam direction and perpendicular to it. As shown in the figure, there are three peaks at the Dy  $M_5$  edge, which are marked by the dashed lines. The maximum XMCD signal appears enhanced at the third peak whereas the maximum XMLD signal is located at the middle peak. The intensity difference at the  $M_5$  edge for the XMLD spectra is sufficiently large to be exploited for intensity measurements as a function of the external field. The sensitivity to the angular orientation between the magnetic moments and the direction of the polarization vector is clearly demonstrated: strong XMLD contrast appears by re-orienting the magnetic moments only, from parallel to perpendicular directions with respect to  $\vec{E}$ , using vectorial magnetic fields. To exclude further contributions to the XMLD contrast possible caused by crystalline electric field effect, further orthogonal field directions in plane of the sample were measured (Supplementary).

To approach the compensation temperature, we performed temperature-dependent XMCD and hysteresis loop measurements at the Dy  $M_{4,5}$  and Co  $L_{2,3}$  edges. Part of the bulk sensitive hysteresis loops taken by measuring the FY intensity at the Dy  $M_5$  edge ( $E = 1298.4$  eV) are shown in Fig. 2. The hysteresis loops signal reverses when the temperature crosses a critical temperature, called magnetic compensation temperature  $T_{comp}$ . Also, the occurrence of the perpendicular magnetic anisotropy is clearly distinguished as the full remanent magnetization and by the sharpness of the magnetization reversal. Besides the main sharp reversal of the film, we observe an

”anomalous” behavior at higher fields which develops at temperatures higher than  $T_{comp}$ . This intriguing response of magnetization at higher magnetic fields is counter-intuitive in nature. For magnetic films which exhibits a net magnetization like ferromagnets, an external field will cause full magnetization, aligning the spins as the field is increased. By contrast, the ”anomalous” hysteresis loop show that the magnetization decreases as the magnetic field is increased.

In Fig. 3(a) we plot the coercive field of the hysteresis loops and the shift of the side hysteresis loops as a function of temperature. The divergence of the coercive field, which occurs at the vanishing net magnetization of the film, reveals with good accuracy the absolute value of the intrinsic  $T_{comp}$  which is about 154 K, in close agreement with previous experiments and simulation results [36, 37]. Also, we plot the field of the center of the wing hysteresis loops as a function of temperature, denoted as exchange bias field  $H_{eb}$ . We observe that the shift of the side loop increases as the temperature increases up to the highest measured value of about 7 T. Due to the finite available external fields (up to 9 T) we could not further follow the shift of the side loop beyond the 7 T. This limitation is visible at 165 K, where the side loop begin to behave as a minor hysteresis loops. Instead, we can determine the limiting temperature where the side loop will vanish. To this end we show in Fig. 3(b) and (c) the inverse of the total net magnetic moments characteristic of bulk and surface, respectively. They are extracted from XMCD spectra measured by TEY and by FY (Supplementary). We observe that both the inverse of the bulk and the surface net magnetic moments exhibit a divergent behaviour, at 154 K for the bulk part of magnetization and at 200 K for the surface part. As such, the system exhibits a different compensation temperature for the probed surface, which is about 50 K higher as compared to the bulk magnetic compensation [24]. In-between these two compensation temperatures the system is in a frustrated state leading to the peculiar wing shape hysteresis loops. The occurrence of these two compensation temperatures correlates very well with the temperature range where the anomalous magnetic behaviour occurs at high fields. Outside this region, we observe no side hysteresis loops because the surface and the bulk spins are in a stable configuration.

To characterize the reversal of the anomalous loops we make use of the XMCD and XMLD effects, focusing on the relevant temperature of 160 K. Fig. 4(a) shows the hysteresis loops at both Dy  $M_5$  edge and Co  $L_3$  edge. They exhibit a similar behaviour with opposite signs. This demonstrates that the magnetic moments of the Dy and Co sublattices are basically anti-parallelly coupled to each other, even when they enter the anomalous spin state at higher fields. At this stage, we can resolute that a spin-flop transition does not occur. Such a spin-flop would appear in the Fig. 4(a) as a significant difference between the shape of the magnetization curves of Dy and Co, which is not observed. However, a weak non-collinear state between Co and Dy net magnetic moments can be distinguished by the difference of the relative magnetizations present at  $\pm 8$  T. This observation is further supported by the demonstration of the same effect in a FeGd film (Supplementary). We can consider that the Co and Dy sublattices are essentially anti-parallelly oriented for all external magnetic fields. This, however, does not exclude a non-collinear behavior for the elemental sublattices: comparing the surface and bulk hysteresis loops, see Fig. 4(b), clearly reveals that the surface signal is almost completely reversed at high fields while the bulk signal is only half reversed, which strongly indicates that the mechanism is due to the reversing of the surface magnetic moments.

By taking advantage of the strong linear dichroism of the Dy element at the  $M_5$  absorption edge, XMLD measurements were applied to understand the anomalous magnetic behavior. Here, we use linear polarized X-rays to perform hysteresis loop measurements, as shown in Fig. 4(c). The XMLD hysteresis loops were recorded at the middle peak of the Dy  $M_5$  edges at  $E = 1296.5$  eV, where we observed a maximum XMLD signal in Fig. 4(d) and Fig. 1(c). From Fig. 4(c) one can see that there are two hysteresis-loop-like structures for both surface and bulk. The two loops appear at the same field of the XMCD ’wing shape’ hysteresis loops but end up at the same level of intensity at  $\pm 8$  T. These results reveal that parts of the magnetic moments rotate from the out-of-plane to the in-plane direction at high fields, which directly indicates the existence of

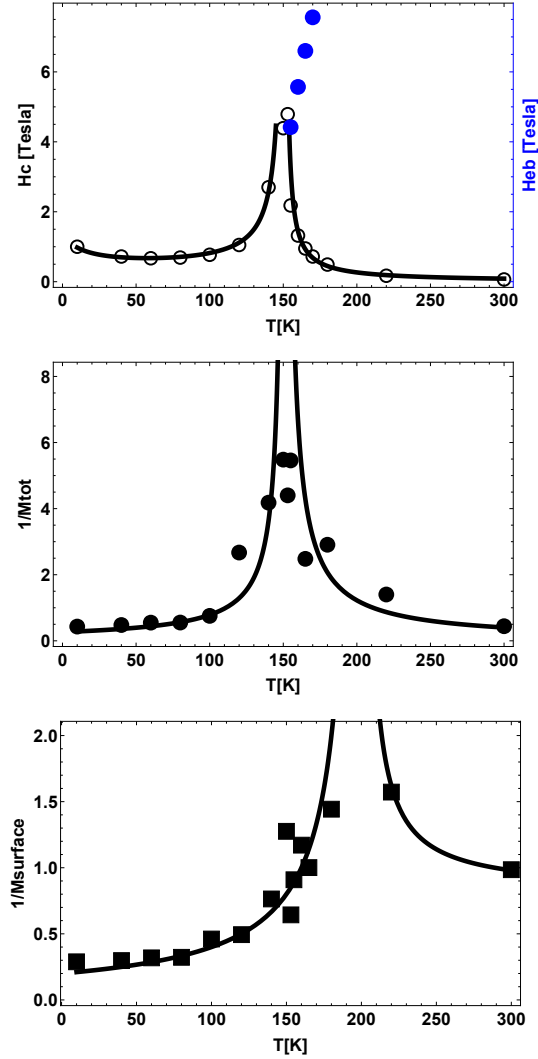


Figure 3: Phase diagram of the magnetic states as a function of temperature: (a) Temperature dependence of the coercivity field  $\mu_0 H_c$  and the exchange bias field  $H_{cb}$ . The values of  $\mu_0 H_c$  were extracted from the rectangular hysteresis loops at the crossing point with respect to the magnetization axis. The shift of the side wings, denoted as  $H_{cb}$ , were extracted at the half height of the side loops alone. The maximum value of  $\mu_0 H_c$  is about 4.8 T slightly below  $T_{comp}$ , whereas the highest measured shift side hysteresis loop is about 7 Tesla; (b) The inverse of the total net magnetic moment extracted by analyzing the XMCD spectra characteristic for the bulk part of the film (FY data). This show a divergent behavior at the closely similar compensation temperature as in panel (a). (c) The inverse of the total net magnetic moment extracted by analyzing the XMCD spectra characteristic for the surface part of the film (TEY data). They also exhibit a divergent behavior near 200 K, showing the probed surface has a higher compensation temperature. In between these two compensation temperatures, the side hysteresis loops occur.

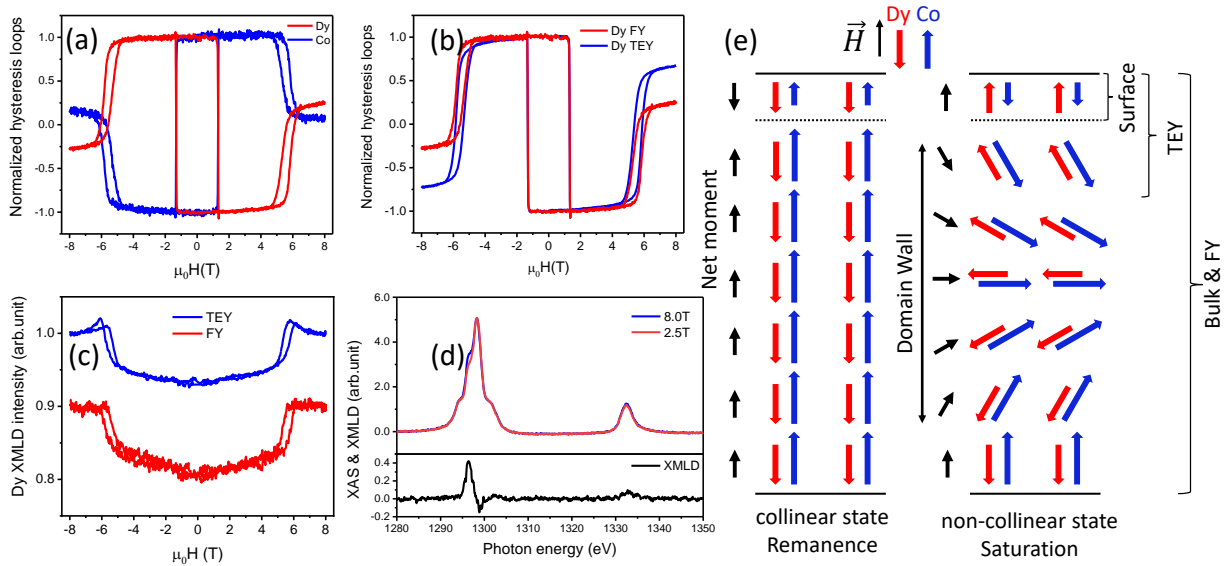


Figure 4: XMCD and XMLD measurements at 160K: (a) Hysteresis loops measured by recording the FY signal with *circular* polarized X-rays at the third peak of the Dy  $M_5$  edges ( $E = 1298.4$  eV) and the Co  $L_3$  edge ( $E = 777.0$  eV). (b) Comparison of surface (TEY) and bulk (FY) hysteresis loops for Dy. (c) XMLD hysteresis loops measured by recording the FY and TEY signal with *linear* polarized X-rays at the second peak of the Dy  $M_5$  edges ( $E = 1296.5$  eV). (d) XAS and XMLD spectra taken at 8 T and 2.5 T for Dy with linear polarized X-rays. (e) Sketch of the magnetic spin structure for the remanence and saturation state.

non-collinear spin structure between the surface and the bulk. One needs to point out that there are also significant differences between the bulk and surface signals. The surface XMLD hysteresis loop reaches a maximum value around  $\pm 6$  T, indicating that the surface magnetic moments rotate to the in-plane direction around this field, then decreases and approaches flattening near  $\pm 8$  T. This further indicates that the surface magnetic moments have a higher rotation angle at high fields. This is in full agreement with a simple domain wall structure initiated at the surface of the film.

Figure 4(d) shows the XAS spectra of Dy and their difference taken at 8 T and 2.5 T with linear polarized X-rays. By comparing the image with the standard XAS and XMLD measurements at 300 K, one can see that the XAS at 8 T is similar to the  $\sigma_{\parallel}$  XAS while the XAS at 2.5 T is close to the  $\sigma_{\perp}$  XAS in Fig. 1(c). By defining the relative XMLD amplitude as  $(\sigma_{\parallel} - \sigma_{\perp}) / (\sigma_{\parallel} + \sigma_{\perp})$ , we get a value of  $\sim 4.4\%$  here and  $\sim 5.6\%$  at 300 K. Note that the XMLD amplitude is believed to be proportional to the square of the total magnetic moments  $M^2$  [29]. The magnetic moments at 160 K are about  $m_{bulk}^{160K} = m_s + m_l = 6.8\mu_B/\text{atom}$  and  $m_{surface}^{160K} = 5.7\mu_B/\text{atom}$ , which are about 1.45 times of the magnetic moments at 300 K  $m_{bulk}^{300K} = 4.8\mu_B/\text{atom}$  and  $m_{surface}^{300K} = 3.8\mu_B/\text{atom}$ . Thus the relative XMLD amplitude of  $5.6\% \times 1.45^2 = 11.6\%$  can be expected at 160 K for the situation that all the magnetic moments align in-plane versus out-of-plane. Here the experimental value of 4.4% means that the in-plane contribution at 8 T is about  $\sqrt{4.4\% / 11.6\%} \approx 62\%$  of the total magnetic moment, which indicates a very thick domain wall probably throughout the whole film.

## Discussion

Based on the experimental facts, one can draw a sketch of the spin structure for the anomalous magnetic behaviour, as shown in Fig. 4(e). The surface magnetic moments are always smaller than the bulk magnetic moments for both Dy and Co. At the magnetic remanence, the spins of

Dy and Co are in a collinear state and anti-parallelly coupled to each other. Due to the strong exchange coupling between the surface and bulk, and due to the fact that the surface magnetism is dominated by Dy while the bulk magnetism is dominated by Co, the net moments of the surface would prefer to align anti-parallel towards the bulk moments. At high fields, this frustrated state becomes unstable, which forces the spin structure of the whole system to turn into a non-collinear state with an out-of-plane partial domain wall. Within this wall, the exchange energy is stored and released, which resembles closely exchange bias interactions with the difference that the atomic exchange is not affected by additional interfaces in an otherwise generic "two magnetic layers" system. By analyzing the net magnetic moments for the bulk and surface, separately, one can localize the temperature range where the occurrence of the side loop takes place. Within this temperature range the shift of the side loop increases as a function of temperature. This can be understood within the general theories for exchange bias [38], which postulates the shift of the hysteresis loop is inverse proportional to the  $M \times t$ , where  $M$  is the magnetization of the active magnetic layer and  $t$  is its thickness. In our case the active layer is the surface which has a compensation temperature of 200 K, therefore, when approaching this temperature the shift of the hysteresis should increase, as observed experimentally in Fig. 3.

To suggest that this effect is a general phenomenon which occurs in thin ferrimagnetic films close to the compensation temperature, we provide supplementary data (Supplementary) on yet another system, namely FeGd ferrimagnetic film. There, the same effects are observed. Nevertheless, since FeGd has a lower magnetic anisotropy and stiffness (due to the nearly vanishing moment of Gd), the temperature range where the shift of the hysteresis loop occurs is larger.

At a more general level, we speculate that our observations may have an impact towards deeper understanding of key aspects of ultrafast magnetic switching in ferrimagnetic films [8, 17]. The mere occurrence of two compensation temperatures comprising two magnetic states in a frustrated arrangement should motivate further experiments which includes this peculiar phase diagram, also considering thickness [39] as a control parameter. As an alternative mechanism for the all optical switching, measured from below compensation in an external field, we can assume an intersection between the intrinsic dynamical paths and the static ones. For instance, if the  $H_{eb}$  will scale down in the non-equilibrium state during the pump probe delay, one can transiently cross over the formation of the domain wall state leading to the so called transient-ferromagnetic state observed for an FeCoGd film in [17]. In fact, strong evidence for this scenario is seen in the Figure S5(a) (Supplementary). There, we observe that the regions between the -6 T and -2 and between 2 T and 6 T are very similar to the so called transient ferromagnetic-like state observed in all optical switching experiments on FeCoGd samples. The projection of the Gd magnetization on the field direction is opposite (after a crossing field equal to 3.5 T) with respect to the magnetization at magnetic remanence, whereas the projection of Fe sublattice magnetization is vanishing. As such, the total net magnetic moment of the whole film is oppositely oriented at high fields (larger than 3.5 T) with respect to the net magnetic moment in lower applied fields (smaller than 3.5 T). Thus, assuming that during the pump probe delay, the time-dependent non-equilibrium states causes the system to cross the critical field for the formation of this "spring" spin configuration, one can understand the origin of the all optical switching in ferrimagnetic thin films by analogy to the effect we reported here. Note, that this mechanism excludes the occurrence of the same all optical switching effect in ferromagnetic materials, because this magnetic spring does not occur in these materials. Instead, the thermally assisted all-optical switching may (disjunctively from the effect we report) take place in ferromagnetic as well as in ferrimagnetic materials as considered in [40, 41].

In conclusion, DyCo<sub>5</sub> ferrimagnetic thin films were investigated with XMLD and XMCD techniques. An anomalous 'wing shape' hysteresis loop, referred to as atomic exchange bias effect with a large exchange bias field of  $\mu_0 H_{EB}$  up to a maximum measurable value of 7 Tesla, was observed slightly above the compensation temperature  $T_{comp} \approx 154$  K. The origin of this effect which is demonstrated to be mediated by the formation of an out-of-plane partial domain wall



during the hysteresis measurements, is directly confirmed via XMLD measurements. Such a huge perpendicular exchange bias effect in a single film may be a good candidate for future perpendicular magnetic recording applications. The technique of using the XMLD contrast at the rare earth  $M_{4,5}$  edges to probe the non-collinear states could be very useful for characterization of non-collinear magnetism which is intimately related to the spintronics research field.

## Methods

### Sample preparation

The 20 nm thick  $DyCo_5$  thin films were grown on sapphire substrates by magnetron sputtering (MAGSSY chamber at HZB) in an ultra-clean Argon atmosphere of  $1.5 \times 10^{-3}$  mbar with a base pressure of  $< 2 \times 10^{-8}$  mbar at room temperature. The stoichiometry of the ferrimagnetic alloy was controlled by varying the deposition rate of Co and Dy targets in a co-evaporation scheme. A 3 nm Ta capping layer was grown on top of the samples to prevent surface oxidation. We have characterized the lateral homogeneity using energy dispersive scanning X-Ray spectroscopy technique (EDS), but were unable to observe any phase separation at the sensitivity level of about few hundred nanometers provided by this method.

### X-ray absorption spectroscopy

The XAS measurements were performed at the VEKMAG end-station [42] installed at the PM2 beamline of the synchrotron facility BESSY II. This end station offers unique capabilities for this type of research, since it provides a vector magnetic field option with a maximum magnetic field up to 9 Tesla in the beam direction, 2 Tesla in the horizontal plane and 1 Tesla in all directions for a temperature range of 2 K - 500 K. The XAS spectra were recorded by means of total electron yield (TEY) and by fluorescence yield (FY), and for each constituent element, separately.

The TEY is measured by recording the drain current as a function of the x-ray photon energy normalized by a Pt grid x-ray monitor mounted in a magnetically shielded environment as the last optical element before the sample. The TEY is known to be surface sensitive, providing information over the escape length of the electrons which exhibits a mean free path of about 3 nm. As such, the surface magnetic properties are provided in a selective manner by this recording channel.

The FY is measured by a magnetically insensitive x-ray detector, placed at 2 cm away from the sample surface. FY is a photon-in photon-out spectroscopic technique which provides information integrated over the penetration depth of the x-ray, which can be of order of tens of nm. The depth sensitivity depends on the photon energy, absorption cross-section, and on the stoichiometry of the film. As such, the FY provides magnetic information for the whole film thickness, which we denote as "bulk" sensitive. The spectra are recorded as function of the x-ray energy and normalized by the same magnetically shielded x-ray monitor.

## References

- [1] V. Baltz, A. Manchon, M. Tsoi, T. Moriyama, T. Ono, and Y. Tserkovnyak. Antiferromagnetic spintronics. *Rev. Mod. Phys.*, 90:015005, Feb 2018.
- [2] Naoto Nagaosa, Jairo Sinova, Shigeki Onoda, A. H. MacDonald, and N. P. Ong. Anomalous hall effect. *Rev. Mod. Phys.*, 82:1539–1592, May 2010.
- [3] Jairo Sinova, Sergio O. Valenzuela, J. Wunderlich, C. H. Back, and T. Jungwirth. Spin hall effects. *Rev. Mod. Phys.*, 87:1213–1260, Oct 2015.

- [4] Florin Radu and Jaime Sánchez-Barriga. Chapter 9 - ferrimagnetic heterostructures for applications in magnetic recording. volume 1 of *Novel Magnetic Nanostructures*, pages 1–70. Elsevier, 2018.
- [5] F Radu, R Abrudan, I Radu, D Schmitz, and H Zabel. Perpendicular exchange bias in ferrimagnetic spin valves. *Nature communications*, 3:715, 2012.
- [6] Mykola Krupa and Andrii Korostil. Pulsed laser impact on ferrimagnetic nanostructures. *International Journal of Physics*, 1(2):28 – 40, 2013.
- [7] A. A. Ünal, S. Valencia, F. Radu, D. Marchenko, K. J. Merazzo, M. Vázquez, and J. Sánchez-Barriga. Ferrimagnetic  $\text{dyco}_5$  nanostructures for bits in heat-assisted magnetic recording. *Phys. Rev. Applied*, 5:064007, Jun 2016.
- [8] C. D. Stanciu, F. Hansteen, A. V. Kimel, A. Kirilyuk, A. Tsukamoto, A. Itoh, and Th. Rasing. All-optical magnetic recording with circularly polarized light. *Phys. Rev. Lett.*, 99:047601, Jul 2007.
- [9] Jun-Yang Chen, Li He, Jian-Ping Wang, and Mo Li. All-optical switching of magnetic tunnel junctions with single subpicosecond laser pulses. *Phys. Rev. Applied*, 7:021001, Feb 2017.
- [10] Sabine Alebrand, Matthias Gottwald, Michel Hehn, Daniel Steil, Mirko Cinchetti, Daniel Lacour, Eric E. Fullerton, Martin Aeschlimann, and Stéphane Mangin. Light-induced magnetization reversal of high-anisotropy tbcO alloy films. *Applied Physics Letters*, 101(16):162408, 2012.
- [11] Ashima Arora, Mohamad-Assaad Mawass, Oliver Sandig, Chen Luo, Ahmet A Ünal, Florin Radu, Sergio Valencia, and Florian Kronast. Spatially resolved investigation of all optical magnetization switching in tbcO alloys. *Scientific reports*, 7:9456, 2017.
- [12] Karel Carva, Pavel Baláž, and Ilie Radu. Chapter 2 - laser-induced ultrafast magnetic phenomena. volume 26 of *Handbook of Magnetic Materials*, pages 291 – 463. Elsevier, 2017.
- [13] M. Binder, A. Weber, O. Mosendz, G. Woltersdorf, M. Izquierdo, I. Neudecker, J. R. Dahn, T. D. Hatchard, J.-U. Thiele, C. H. Back, and M. R. Scheinfein. Magnetization dynamics of the ferrimagnet  $\text{Co}_2\text{FeSi}$  near the compensation of magnetization and angular momentum. *Phys. Rev. B*, 74:134404, Oct 2006.
- [14] Kab-Jin Kim, Se Kwon Kim, Yuushou Hirata, Se-Hyeok Oh, Takayuki Tono, Duck-Ho Kim, Takaya Okuno, Woo Seung Ham, Sanghoon Kim, Gyoungchoon Go, Yaroslav Tserkovnyak, Arata Tsukamoto, Takahiro Moriyama, Kyung-Jin Lee, and Teruo Ono. Fast domain wall motion in the vicinity of the angular momentum compensation temperature of ferrimagnets. *Nature Materials*, 16:1187 EP –, Sep 2017.
- [15] Christian Kaiser, Alex F. Panchula, and Stuart S. P. Parkin. Finite tunneling spin polarization at the compensation point of rare-earth-metal/transition-metal alloys. *Phys. Rev. Lett.*, 95:047202, Jul 2005.
- [16] C. D. Stanciu, A. Tsukamoto, A. V. Kimel, F. Hansteen, A. Kirilyuk, A. Itoh, and Th. Rasing. Subpicosecond magnetization reversal across ferrimagnetic compensation points. *Phys. Rev. Lett.*, 99:217204, Nov 2007.
- [17] I Radu, K Vahaplar, C Stamm, T Kachel, N Pontius, HA Dürr, TA Ostler, J Barker, RFL Evans, RW Chantrell, et al. Transient ferromagnetic-like state mediating ultrafast reversal of antiferromagnetically coupled spins. *Nature*, 472(7342):205–208, 2011.

- [18] TA Ostler, J Barker, RFL Evans, RW Chantrell, U Atxitia, O Chubykalo-Fesenko, S El Mousaoui, LBPJ Le Guyader, E Mengotti, LJ Heyderman, et al. Ultrafast heating as a sufficient stimulus for magnetization reversal in a ferrimagnet. *Nature communications*, 3:666, 2012.
- [19] Roshnee Sahoo, Lukas Wollmann, Susanne Selle, Thomas Hche, Benedikt Ernst, Adel Kalache, Chandra Shekhar, Nitesh Kumar, Stanislav Chadov, Claudia Felser, Stuart S. P. Parkin, and Ajaya K. Nayak. Compensated ferrimagnetic tetragonal heusler thin films for antiferromagnetic spintronics. *Advanced Materials*, 28(38):8499–8504, 2016.
- [20] Sotaro Esho. Anomalous magneto-optical hysteresis loops of sputtered gd-co films. *Japanese Journal of Applied Physics*, 15(S1):93, 1976.
- [21] Ratajczak H. and Gošciańska I. Hall hysteresis loops in the vicinity of compensation temperature in amorphous hoco films. *physica status solidi (a)*, 62(1):163–168.
- [22] Tu Chen and R. Malmhll. Anomalous hysteresis loops in single and double layer sputtered tbfe films. *Journal of Magnetism and Magnetic Materials*, 35(1):269 – 271, 1983.
- [23] Kensho Okamoto and Noboru Miura. Hall effect in a re-tm perpendicular magnetic anisotropy film under pulsed high magnetic fields. *Physica B: Condensed Matter*, 155(1):259 – 262, 1989.
- [24] Kai Chen, Dieter Lott, Florin Radu, Fadi Choueikani, Edwige Otero, and Philippe Ohresser. Observation of an atomic exchange bias effect in dyco4 film. *Scientific reports*, 5, 2015.
- [25] M. Amatsu, S. Honda, and T. Kusuda. Anomalous hysteresis loops and domain observation in gd-fe co-evaporated films. *IEEE Transactions on Magnetics*, 13(5):1612–1614, Sep 1977.
- [26] Chudong Xu, Zhifeng Chen, Daxin Chen, Shiming Zhou, and Tianshu Lai. Origin of anomalous hysteresis loops induced by femtosecond laser pulses in gdfeco amorphous films. *Applied Physics Letters*, 96(9):092514, 2010.
- [27] J. Becker, A. Tsukamoto, A. Kirilyuk, J. C. Maan, Th. Rasing, P. C. M. Christianen, and A. V. Kimel. Ultrafast magnetism of a ferrimagnet across the spin-flop transition in high magnetic fields. *Phys. Rev. Lett.*, 118:117203, Mar 2017.
- [28] G. Schütz, W. Wagner, W. Wilhelm, P. Kienle, R. Zeller, R. Frahm, and G. Materlik. Absorption of circularly polarized x rays in iron. *Phys. Rev. Lett.*, 58:737–740, Feb 1987.
- [29] B. T. Thole, G. van der Laan, and G. A. Sawatzky. Strong magnetic dichroism predicted in the  $M_{4,5}$  x-ray absorption spectra of magnetic rare-earth materials. *Phys. Rev. Lett.*, 55:2086–2088, Nov 1985.
- [30] Pieter Kuiper, Barry G. Searle, Petra Rudolf, L. H. Tjeng, and C. T. Chen. X-ray magnetic dichroism of antiferromagnet  $fe_2o_3$ : The orientation of magnetic moments observed by fe 2p x-ray absorption spectroscopy. *Phys. Rev. Lett.*, 70:1549–1552, Mar 1993.
- [31] Gerrit van der Laan. Magnetic linear x-ray dichroism as a probe of the magnetocrystalline anisotropy. *Phys. Rev. Lett.*, 82:640–643, Jan 1999.
- [32] S. S. Dhesi, G. van der Laan, and E. Dudzik. Determining element-specific magnetocrystalline anisotropies using x-ray magnetic linear dichroism. *Applied Physics Letters*, 80(9):1613–1615, 2002.
- [33] Elke Arenholz, Gerrit van der Laan, Rajesh V. Chopdekar, and Yuri Suzuki. Angle-dependent  $ni^{2+}$  x-ray magnetic linear dichroism: Interfacial coupling revisited. *Phys. Rev. Lett.*, 98:197201, May 2007.

- [34] Elke Arenholz, Gerrit van der Laan, Rajesh V. Chopdekar, and Yuri Suzuki. Anisotropic x-ray magnetic linear dichroism at the fe  $L_{2,3}$  edges in  $fe_3o_4$ . *Phys. Rev. B*, 74:094407, Sep 2006.
- [35] A Ruosi, C Raisch, A Verna, R Werner, BA Davidson, J Fujii, R Kleiner, and D Koelle. Electron sampling depth and saturation effects in perovskite films investigated by soft x-ray absorption spectroscopy. *Physical Review B*, 90(12):125120, 2014.
- [36] T. Tsushima and M. Ohokoshi. Spin reorientation in dyco5. *Journal of Magnetism and Magnetic Materials*, 31-34:197 – 198, 1983.
- [37] Andreas Donges, Sergii Khmelevskiy, Andras Deak, Radu-Marius Abrudan, Detlef Schmitz, Ilie Radu, Florin Radu, László Szunyogh, and Ulrich Nowak. Magnetization compensation and spin reorientation transition in ferrimagnetic dyco<sub>5</sub>: Multiscale modeling and element-specific measurements. *Phys. Rev. B*, 96:024412, Jul 2017.
- [38] Florin Radu and Hartmut Zabel. *Exchange Bias Effect of Ferro-/Antiferromagnetic Heterostructures*, pages 97–184. Springer Berlin Heidelberg, Berlin, Heidelberg, 2008.
- [39] Ashima Arora, Mohamad-Assaad Mawass, Oliver Sandig, Chen Luo, Ahmet A. Ünal, Florin Radu, Sergio Valencia, and Florian Kronast. Spatially resolved investigation of all optical magnetization switching in tbfe alloys. *Scientific Reports*, 7(1):9456, 2017.
- [40] S. Mangin, M. Gottwald, C.-H. Lambert, D. Steil, V. Uhlír, L. Pang, M. Hehn, S. Alebrand, M. Cinchetti, G. Malinowski, Y. Fainman, M. Aeschlimann, and E. E. Fullerton. Engineered materials for all-optical helicity-dependent magnetic switching. *Nature Materials*, 13:286 EP –, Feb 2014. Article.
- [41] Alexander Hassdenteufel, Birgit Hebler, Christian Schubert, Andreas Liebig, Martin Teich, Manfred Helm, Martin Aeschlimann, Manfred Albrecht, and Rudolf Bratschitsch. Thermally assisted all-optical helicity dependent magnetic switching in amorphous fe100xtbx alloy films. *Advanced Materials*, 25(22):3122–3128.
- [42] T. Noll and F. Radu. The mechanics of the vekmag experiment. In Volker RW Schaa, editor, *Proc. of MEDSI2016, Barcelona, Spain, September 11?16, 2016*, number Geneva, Switzerland in 9, pages 370–373. JACoW, 2017.

## Acknowledgments

The x-ray absorption measurements were carried out at the VEK MAG end-station installed at the PM2-VEK MAG beamlines, of BESSY II, Helmholtz-Zentrum Berlin (HZB). We thank the HZB for the allocation of synchrotron radiation beamtime. The authors acknowledge the financial support for the VEK MAG project and for the PM2-VEK MAG beamline by the German Federal Ministry for Education and Research (BMBF 05K10PC2, 05K10WR1, 05K10KE1) and by HZB. Steffen Rudorff is acknowledged for technical support.

Supplementary information for:

# X-ray magnetic linear dichroism as a probe for non-collinear magnetic state in ferrimagnetic single layer exchange bias systems

Chen Luo<sup>1,2,3,\*</sup>, Hanjo Ryll<sup>1</sup>, Christian H. Back<sup>2,3</sup>, and Florin Radu<sup>1,\*\*</sup>

<sup>1</sup>Helmholtz-Zentrum-Berlin für Materialien und Energie, Albert-Einstein-Strasse 15, 12489 Berlin, Germany

<sup>2</sup>Institute of Experimental and Applied Physics, University of Regensburg, 93053 Regensburg, Germany

<sup>3</sup>Institute of Experimental Physics of Functional Spin Systems, Technical University Munich, James-Frank-Str. 1, 85748 Garching b. München, Germany

\* *chen.luo@ur.de*

\*\* *florin.radu@helmholtz-berlin.de*

November 14, 2018

## Supplementary Notes

### S1 XMLD: experimental geometries utilizing vectorial magnetic fields

We describe below the experimental geometries for the linear dichroism measurements using vector magnetic fields on the Ta/DyCo<sub>5</sub>/Al<sub>2</sub>O<sub>3</sub> sample of the main body of the paper. This demonstrates in a self-consistent manner the sensitivity of the XMLD contrast to the angle of magnetization direction with respect to the direction of the linear polarization. There are two common ways to measure a XMLD spectra. One is to keep the magnetization along the easy direction and to rotate the polarization direction, the other one is to keep the linear polarization direction fixed and change the magnetization direction [1]. Here, by taking advantage of the 3D vector magnet of the VEKMAG end-station, the second method is being used for our measurements. We set the linear polarization  $\vec{E}$  oriented perpendicular to the beam direction and parallel to the storage ring plane. The sample is oriented perpendicular to the beam direction, as for transmission geometry. The magnetization of the sample is set oriented by the external field in three orthogonal directions:  $H_{IP}^{\parallel}$ ,  $H_{IP}^{\perp}$ , and  $H_{OP}^{\perp}$ , as shown in Fig. S1(a). The *OP* and *IP* indexes refer to the direction of the magnetization with respect to the sample, namely out-of-plane and in-plane, respectively. The  $\parallel$  and  $\perp$  indexes refer to the orientation of the magnetization with respect to the linear polarization direction of the X-rays, namely parallel or perpendicular to  $\vec{E}$ , respectively.

The XAS spectra and their difference are shown in Fig. S1(b,c,d). The difference between the spectra measured for the orthogonal directions  $H_{IP}^{\parallel}$  and  $H_{OP}^{\perp}$ , as well as for  $H_{IP}^{\parallel}$  and  $H_{IP}^{\perp}$ , do show a XMLD contrast (black line in Fig. S1(c,d)). By contrast, when we compare the spectra recorded for  $H_{IP}^{\perp}$  and  $H_{OP}^{\perp}$ , we observe a vanishing XMLD contrast (black line in Fig. S1(b)). This demonstrates that the XMLD contrast is sensitive only to the orientation between the direction of magnetization with respect to the direction of the linear polarization. Given that the amplitude of the XMLD is large, reaching a  $\sim 5.6\%$  at room temperature, the intensity difference at the middle peak of the  $M_5$  edge, allows for detecting non-collinearity between the magnetization and the direction of the external field during hysteresis measurements, as described in the main body of the paper.

arXiv:1811.05362v1 [cond-mat.mtrl-sci] 13 Nov 2018

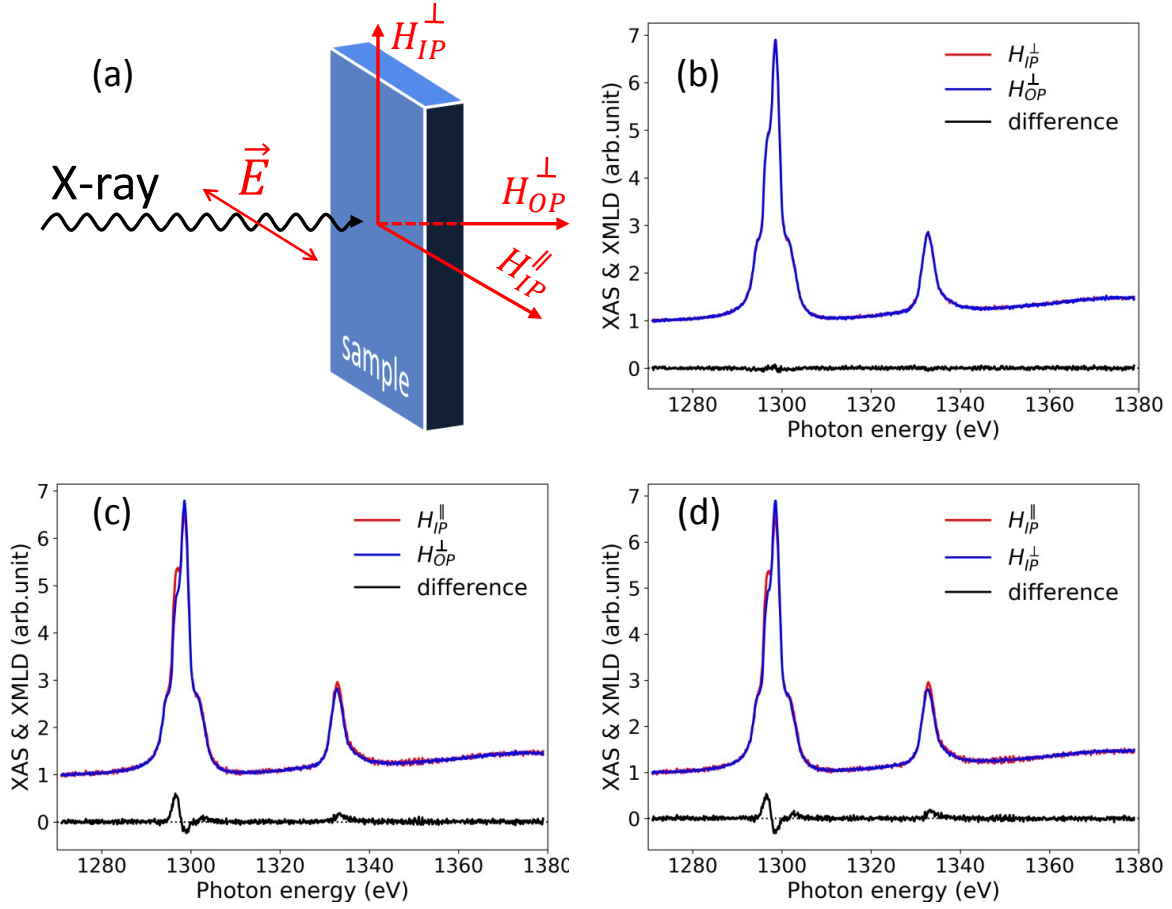


Figure S1: (a) Sketch of the XMLD measurements at room temperature. Here  $H_{IP}^{\parallel}$  represents the field direction which lies in-plane and parallel to the  $\vec{E}$  vector of the linear polarized X-rays,  $H_{IP}^{\perp}$  represents the field direction which lies in-plane and perpendicular to  $\vec{E}$ , and  $H_{OP}^{\perp}$  is the out-of-plane direction (perpendicular to the  $\vec{E}$ ). (b,c,d) show the XAS spectra measured at  $H_{IP}^{\parallel}$ ,  $H_{IP}^{\perp}$  and  $H_{OP}^{\perp}$ , as well as their differences. The XAS spectra were measured by recording the FY as a function of x-ray energy across the  $M_5$  and  $M_4$  edges of Dy.

## S2 XMCD: analysis of the magnetic moments

Due to the existence of the self-absorption and radiative decay effects, the FY spectra may exhibit a nonlinear dependence with respect to the absorption cross section [?, 2, 3]. To compare the difference between the XMCD measured in FY, TEY and transmission mode, we prepared a calibration sample Ta(2.5 nm)/DyCo<sub>5</sub>(20 nm)/Ta(5 nm) grown on a 150 nm thick Si<sub>3</sub>N<sub>4</sub> membrane substrate. This allows us to measure the XAS and XMCD using TEY, fluorescence and transmission signals at the same time, as shown in Figure S2 (a,b,c). For a direct comparison, we have re-plotted all three XMCD spectra in Figure S2 (d). Comparing the XMCD spectra measured in transmission with the XMCD spectra measured in TEY mode, we observe that they have an identical line shape, with a clear difference in amplitude. This directly demonstrates that the magnetic moments of the surface are smaller as compared to the magnetic moments of the bulk part. However, the magnetic moments of the bulk measured by transmission and FY should have the same amplitude, which should be reflected in a similar amplitude and line-shape for the XMCD spectra. This is, however, not the case as directly demonstrated in Figure S2 (d): the amplitude of the XMCD spectra is similar for the transmission and FY modes, but the XMCD line-shape measured by FY exhibits an enhanced spectral feature at 1294.3 eV. This difference prevents an accurate determination of the spin and orbital moments through FY measurements. Nevertheless, we have applied the sum rules to the FY and transmission XMCD spectra and obtained the following magnetic moments at room temperature:  $m_{total}^{FY} = 4.8\mu_B/\text{atom}$  and  $m_{total}^{TR} = 3.9\mu_B/\text{atom}$ . One can see that the magnetic moment obtained from the fluorescence spectra is about 23% larger as compared to the value from the transmission spectra.

We then further use this scaling factor to correct for the magnetic moments extracted by applying the sum rules to the temperature dependence of the Dy XMCD spectra measured by FY in the main paper. For XMCD measured by FY for Co (not shown), this factor turned out to close to 1. We observe that both Co and Dy exhibit lower moments on the surface for the whole temperature range, with different percentages: the Co surface has about 67% of the bulk net moment value, whereas the Dy surface has about 84% of its bulk value. The fact that the Co moment is reduced stronger as compare to the Dy moment may indicate a non-collinear arrangement between the Co and the Dy spins at the top surface. This can be a result of a reduced surface coordination. The results are plotted in Fig. S3 to serve as the basis for the observed difference between the compensation temperatures of bulk and surface parts of the film.

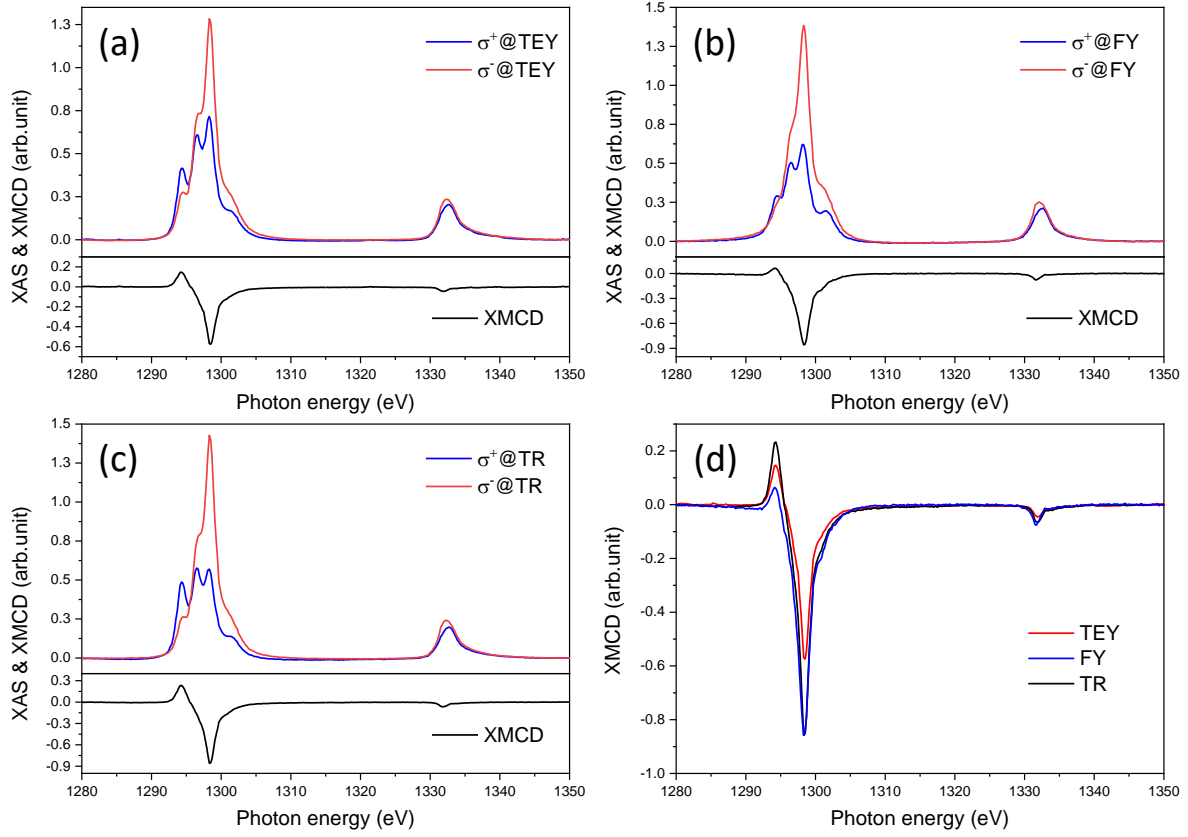


Figure S2: The Dy XAS and XMCD spectra measured by recording the TEY (a), FY (b) and transmission signals (c). (d) Comparison between the TEY, FY and transmission XMCD spectra.

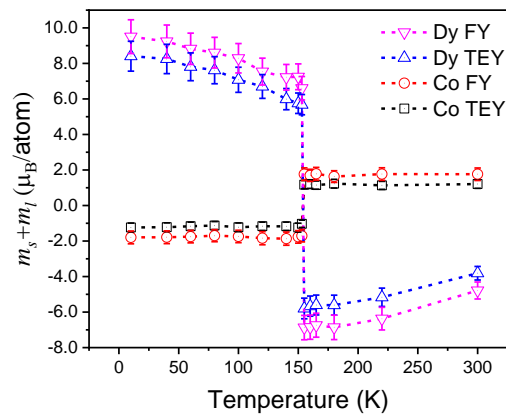


Figure S3: Temperature dependence of the total magnetic moments  $m_s + m_l$ . The spin  $m_s$  and orbital  $m_l$  magnetic moments were obtained by applying the XMCD sum rules [4, 5, 6] for the XAS and XMCD spectra measured at remanent magnetization. The sign of the magnetic moments reverses after crossing  $T_{comp}$ .



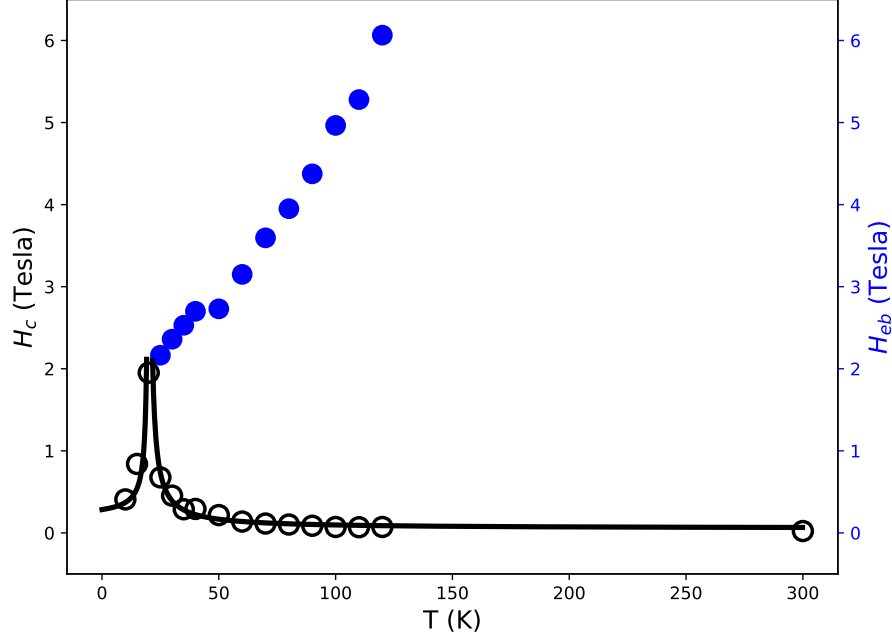


Figure S4: Temperature dependence of the coercive field  $H_c$  (open black circles) and the exchange bias field  $H_{eb}$  (filled blue circles) for an FeGd film. The values of  $H_c$  were extracted from the rectangular hysteresis loops at the crossing point with respect to the magnetization axis. The shift of the side wings, denoted as  $H_{eb}$ , were extracted at the half height of the side loops alone. The maximum value of  $H_c$  is about 2 T slightly aside  $T_{comp}$ , whereas the highest measured shift of the side hysteresis loop is about 6.2 Tesla. The lines are guides to the eyes.

### S3 Support study of the atomic exchange bias in FeGd film

For the purpose of supporting our results and method, and to demonstrate a general character of our observations, we show one more model system, namely a FeGd ferrimagnetic thin film. The sample has the following structure Ta(2.5 nm)/Fe<sub>77</sub>Gd<sub>23</sub> (20 nm)/Ta(5 nm)/Si<sub>3</sub>N<sub>4</sub>. The Gd layer exhibits a nearly vanishing orbital magnetic moment, therefore the magnetic anisotropy and the stiffness of the film are much lower as compared to the Dy based alloys. As such it can be used as soft magnetic element in ferrimagnetic spin valves and it is the preferred system for the all optical ultrafast magnetic switching effect.

In Figure S4 we show the dependence of the coercive field and the shift of the side loop as a function of temperature. The coercive field exhibits a typical divergent behaviour at the compensation temperature which for this sample is about 25 K. Above the compensation temperature, the system develops an additional hysteresis loop denoted as  $H_{eb}$  which increases steadily up to a maximum measured value of about 6.2 T. Comparing this phase diagram with the one of DyCo<sub>5</sub> film we notice a similar character, but with some markedly differences: the temperature range where the atomic exchange bias occur is larger for FeGd (more 100 K) as compared to DyCo<sub>5</sub>. Also, the temperature dependence of the  $H_{eb}$  shows deviations from a linear behaviour which is actually expected within the theories of exchange bias effect. Note that for the FeGd samples we did not measure the magnetic moments, as such we cannot provide the exact compensation temperature of the surface part.

In Figure S5 we provide an overview of the magnetic behaviour for a constant temperature equal to 35 K. The sample has been measured in transmission and TEY modes. The element

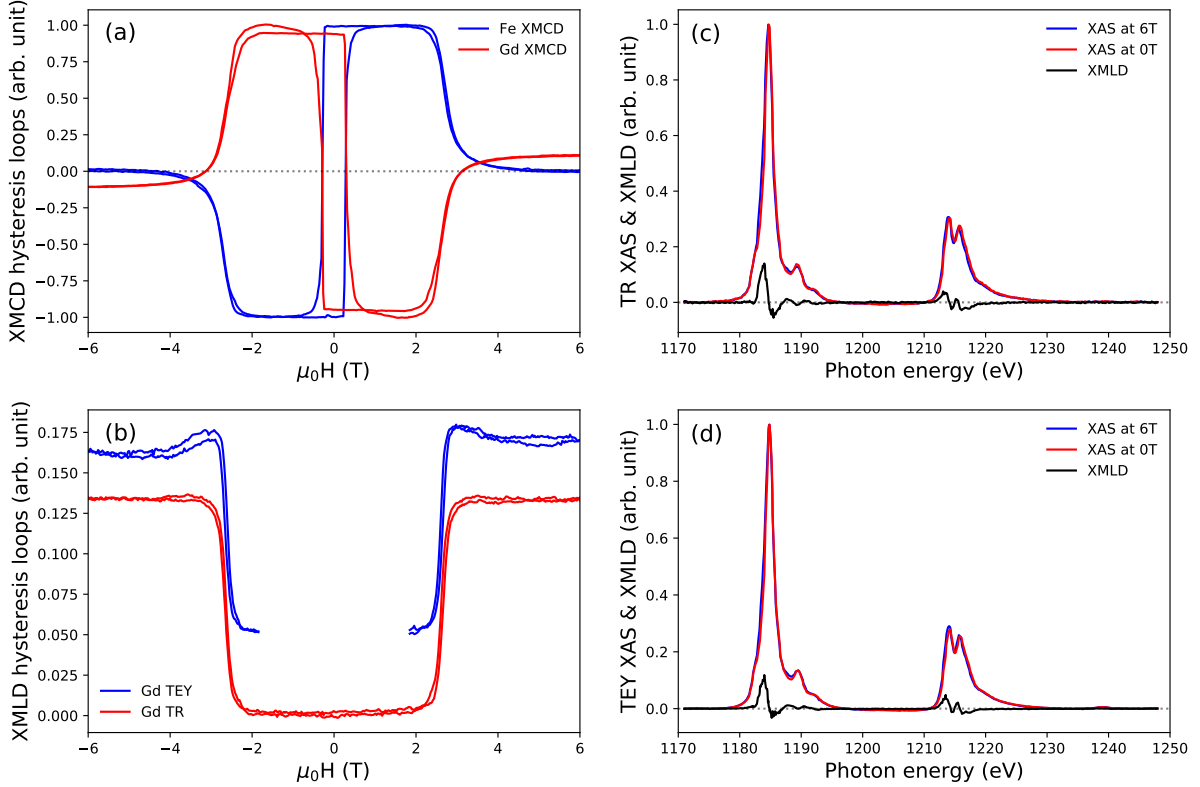


Figure S5: (a) The out-of-plane XMCD hysteresis loops are measured by recording the transmission signals with *circular* polarized X-rays at the Gd  $M_5$  edge  $E = 1184.9$  eV and at Fe  $L_3$  edge  $E = 707$  eV. They clearly demonstrate that the magnetic moments of the Gd and Fe are coupled anti-parallel one to each other. (b) The XMLD hysteresis loops are measured using the *linear* polarized X-rays at the Gd  $M_5$  edge  $E = 1183.7$  eV. Note that, for the TEY loop the data at smaller fields are not shown due to a common artefact caused by the electrons near zero field during field sweep measurements, leading to large distortions of the curve. (c,d) The XAS and XMLD spectra measured at 0T and 6T. Here we observe a  $\approx 13.5\%$  XMLD signal for transmission (c) and  $\approx 10.6\%$  for TEY (d).

specific (for Fe  $L_3$  and Gd  $M_5$  edges) magnetic hysteresis loops (Figure S5(a)) were measured in transmission mode (bulk part) with circular polarized beam (XMCD) impinging perpendicular to the sample surface. They display a central rectangular loop which is characteristic for the perpendicular anisotropy, and the side loops. These hysteresis loops clearly show that the Fe and Gd sub-lattice magnetizations are anti-parallelly oriented with respect to one another. At the highest fields, one notices that a weak non-collinearity occurs. Strikingly, the regions between the -6 T and -2 T and between 2 T and 6 T are very similar to the so called transient ferromagnetic-like state observed in all optical switching experiments on FeCoGd samples [7] (see also the Discussion section in the main manuscript).

The hysteresis loops with linear polarization (XMLD) for both the surface (TEY) and the bulk (transmission) parts exhibit a clear imprint of a large rotation of the sub-lattices from out-of-plane direction to an in-plane direction (Figure S5(b)). The differences between the surface and the bulk are also clearly observed, suggesting that the surface spins are more susceptible to the external fields. Finally, the XMLD spectra are shown for both TEY and transmission modes in Figure S5(c, d). Similar to Dy, the Gd does also exhibit a large XMLD contrast which can be used for non-collinearity studies.

## References

- [1] Gerrit van der Laan. Magnetic linear x-ray dichroism as a probe of the magnetocrystalline anisotropy. *Phys. Rev. Lett.*, 82:640–643, Jan 1999.
- [2] S. Eisebitt, T. Böske, J.-E. Rubensson, and W. Eberhardt. Determination of absorption coefficients for concentrated samples by fluorescence detection. *Phys. Rev. B*, 47:14103–14109, Jun 1993.
- [3] M. Pompa, A. M. Flank, P. Lagarde, J. C. Rife, I. Stekhin, M. Nakazawa, H. Ogasawara, and A. Kotani. Experimental and theoretical comparison between absorption, total electron yield, and fluorescence spectra of rare-earth  $M_5$  edges. *Phys. Rev. B*, 56:2267–2272, Jul 1997.
- [4] Paolo Carra, B. T. Thole, Massimo Altarelli, and Xindong Wang. X-ray circular dichroism and local magnetic fields. *Phys. Rev. Lett.*, 70:694–697, Feb 1993.
- [5] B. T. Thole, P. Carra, F. Sette, and G. van der Laan. X-ray circular dichroism as a probe of orbital magnetization. *Phys. Rev. Lett.*, 68:1943–1946, Mar 1992.
- [6] C. T. Chen, Y. U. Idzerda, H.-J. Lin, N. V. Smith, G. Meigs, E. Chaban, G. H. Ho, E. Pellegrin, and F. Sette. Experimental confirmation of the x-ray magnetic circular dichroism sum rules for iron and cobalt. *Phys. Rev. Lett.*, 75:152–155, Jul 1995.
- [7] I Radu, K Vahaplar, C Stamm, T Kachel, N Pontius, HA Dürr, TA Ostler, J Barker, RFL Evans, RW Chantrell, et al. Transient ferromagnetic-like state mediating ultrafast reversal of antiferromagnetically coupled spins. *Nature*, 472(7342):205–208, 2011.